ISSN 2522-3488 Vol. 8, Issue 4: 10-15, DOI: 10.25236/IJNDES.2024.080402

Research on Maximum Energy Supply Capacity of Electric-Gas-Thermal Interconnection Integrated Energy System

Wanjia Zhang*, Liang Zhou#, Luqiang Shi#, Baisong Wang#

State Grid Hangzhou Power Supply Company, Hangzhou, 310016, China
Corresponding author: hdzhangwanjia@163.com
#These authors contributed equally.

Abstract: *Considering the equation and inequality constraints of four parts including power system, gas system, thermal system and element output, the paper aims at constructing a multi-scenario Electric-Gas-Thermal interconnection integrated energy system with energy storage elements and wind turbine, which pointing at the maximum energy supply capacity of Electric-Gas-Thermal integrated energy system. The Gurobi solver is invoked in MATLAB to solve the coupling IEEE39- node power system, the 6-node gas system and the 6-node thermal system. The energy supply capacity of normal situation, electric power system N-1 fault scenario, gas system N-1 fault scenario, thermal system N-1 fault scenario are calculated. Measuring the maximum energy supply capacity of the Electric-Gas-Thermal integrated energy system can provide decision support for the safe operation of the integrated energy system. It is more conducive to the reasonable planning of load distribution and the increase of system operation reliability.*

Keywords: *Energy Storage Element, Wind Turbine, Integrated Energy System, Maximum Energy Supply Capacity*

1. Introduction

The traditional energy supply mode is characterized by separation, occupying a significant amount of land, lack of sharing and interconnection, chaotic management, and high cost [1]. On the other hand, the Electric-Gas-Thermal interconnection integrated energy system represents an all-in-one supply mode that enables synergistic interaction between horizontal electric, gas, and thermal energy as well as vertical source, network, load, storage, and utilization [2]. This system exhibits characteristics such as land intensity, equipment intensity, function intensity, and operation intensity [3].

A multitude of coupling devices enhance the coupling between electric, gas, and thermal energy sources while also increasing uncertainty [4]. The calculation of the maximum energy supply capacity of the Electric-Gas-Thermal interconnection integrated energy system is crucial for harnessing the power supply potential of such an integrated energy system [5].

The research on maximum energy supply capacity in power systems is well-established and mature. However, there are limited studies focusing on integrated energy systems with coupled energy sources [6]. Previous literature proposes a calculation model for determining the maximum energy supply capacity in Electric-Gas interconnection System [7].

Based on this premise, this paper constructs a multi-scenario model for determining the maximum energy supply capacity in Electric-Gas-Thermal interconnection integrated energy system. This model incorporates uncertainties associated with energy storage element and wind turbine while obtaining the normal scenario's as well as N-1 fault scenario's power line's respective capacities.

2. Maximum energy capacity model of Electric-Gas-Thermal interconnection integrated energy system

2.1 Objective function

(1) F is the maximum energy supply capacity of the Electric-Gas-Thermal interconnection integrated

ISSN 2522-3488 Vol. 8, Issue 4: 10-15, DOI: 10.25236/IJNDES.2024.080402

energy system, and the minimum value of each scenario is taken.

(2) $F_{scenario}$ is the maximum energy supply capacity under each scenario, which includes three parts: the energy supply capacity of the electric power system under each scenario, the energy supply capacity of the gas system under each scenario, and the energy supply capacity of the thermal system under each scenario.

$$F = \min F_{\text{scenario}}, \tag{1}$$

$$F_{\text{scenario}} = \max(P_{electric} + P_{gas,electric} + P_{thermal}), \tag{2}$$

2.2 Constraint condition

2.2.1 Electric power system constraint

Power balance constraints, including generator generation, wind turbine generation, CHP unit output of electricity, G2P equipment output of electricity, energy storage element discharge and charge, P2G equipment consumption and electricity load. The inequality constraint is the power flow constraint.

$$P_G + P_w + P_{CHP} + P_{G2P} + P_{ES}^{\text{out}} = P_{\text{L}} + P_{P2G} + P_{ES}^{in}, \tag{3}$$

$$P_{ij}^{\min} \le P_{ij} \le P_{ij}^{\max}, \tag{4}$$

2.2.2 Gas system constraint

Gas balance constraints include gas output from natural gas sources, gas output from P2G equipment, gas consumption from CHP units, gas consumption from G2P equipment, and gas load. In this paper, a bidirectional second-order cone-convex relaxation model of natural gas pipeline flow is constructed. In this model, the flow direction of the pipeline is assisted by 0-1 binary variables, which can consider the bidirectional flow of natural gas in the pipeline.

$$Q_{source} + Q_{P2G} = Q_{CHP} + Q_{G2P} + Q_L, \tag{5}$$

2.2.3 Thermal system constraint

Thermal balance constraints include CHP unit thermal production, thermal source thermal production and thermal load. Hydraulic network belongs to fluid network and its model is described by flow continuity equation and loop pressure drop equation. The thermodynamic model is composed of thermal equation, temperature drop equation of pipeline and mixing temperature equation of node.

$$\psi_{CHP} + \psi_{source} = \psi_L, \tag{6}$$

2.2.4 Equipment output constraint

(1) Because the system does not have enough margin to absorb a large amount of wind power during windy periods, wind curtailment may occur, so the wind turbine output will not exceed the maximum output limit[8].

$$0 \le P_w \le P_w^{\max}, \tag{7}$$

(2) The storage battery is charged at valley charge and discharged at peak charge as an auxiliary means to improve the matching degree of source charge. Its model includes the constraint that charge and discharge cannot be carried out simultaneously in the same period, the upper limit of charge and discharge power and the upper limit of capacity[9].

$$\tau_{ES}^{in} + \tau_{ES}^{\text{out}} \le 1, \tag{8}$$

$$\tau_{ES}^{out} P_{ES,\min}^{out} \le P_{ES}^{\text{out}} \le \tau_{ES}^{out} P_{ES,\max}^{out}, \tag{9}$$

$$\tau_{ES}^{in} P_{ES,\min}^{in} \le P_{ES}^{in} \le \tau_{ES}^{in} P_{ES,\max}^{in}, \tag{10}$$

ISSN 2522-3488 Vol. 8, Issue 4: 10-15, DOI: 10.25236/IJNDES.2024.080402

$$S_{ES} = \eta_{ES}^{in} P_{ES}^{in} - \eta_{ES}^{\text{out}} P_{ES}^{out}, \tag{11}$$

$$S_{ES,\min} \le S_{ES} \le S_{ES,\max}, \tag{12}$$

(3) Common thermoelectric coupled CHP units models are as follows.

$$P_{CHP} = \eta_{CHP}^{e} Q_{CHP} \bullet q_{Gas}, \tag{13}$$

$$\psi_{CHP} = \eta_{CHP}^{h} Q_{CHP} \bullet q_{Gas}, \tag{14}$$

(4) The P2G equipment first produces hydrogen through alkaline electrolysis of water, and on the basis of electric conversion to hydrogen, hydrogen and carbon dioxide react under the catalyst to produce methane and water[10].

$$\eta_{P2G} P_{P2G} = Q_{P2G} \bullet q_{Gas}, \tag{15}$$

(5) Common G2P device models are as follows.

$$P_{G2P} = \eta_{G2P} Q_{G2P} \bullet q_{Gas}, \tag{16}$$

3. The process of solving the maximum energy supply capacity of the Electric-Gas-Thermal interconnection integrated energy system

Calling Gurobi solver to solve the maximum energy supply capacity of the Electric-Gas-Thermal interconnection integrated energy system is as follows:

(1) Input power system parameters, gas system parameters, thermal system parameters.

(2) k=0, normal scenario.

(3) Calculate the maximum energy supply capacity when k=0.

(4) k=k+1, perform the scenario in sequence.

(5) Calculate the maximum energy supply capacity at this time.

(6) Whether $\mathrm{k} = \mathrm{k}_{\text{last}}$ is true, if yes, proceed to the next step, no, return to Step(4)continue the calculation. k_{last} is the number of all scenes.

(7) Compare the maximum energy supply capacity of all scenarios, and select the minimum value as the maximum energy supply capacity of the Electric-Gas-Thermal interconnection integrated energy system.

4. Analysis of examples

4.1 Example parameter setting

This paper verifies the feasibility and effectiveness of this model based on the improved IEEE39-node electric power system, 6-node gas system and 6-node thermal system. The topology diagram is shown in Fig 1. The electric power system includes seven generators, one wind turbine, one energy storage element, and 19 electric power system loads. The gas system consists of two gas sources and two gas loads. The thermal system consists of one heat source and three heat loads. The parameters of electric power system are shown in literature [11] and the parameters of gas system and thermal system are shown in literature [12].

Using MATLAB R2016a simulation and calling Gurobi solver, simulation analysis is performed for the following two scenarios:

(1) Normal scenario (electric power system, gas system, thermal system are in normal condition);

(2) Electric power system line N-1 fault scenario.

ISSN 2522-3488 Vol. 8, Issue 4: 10-15, DOI: 10.25236/IJNDES.2024.080402

(3) Gas system line N-1 fault scenario.

(4) Thermal system line N-1 fault scenario.

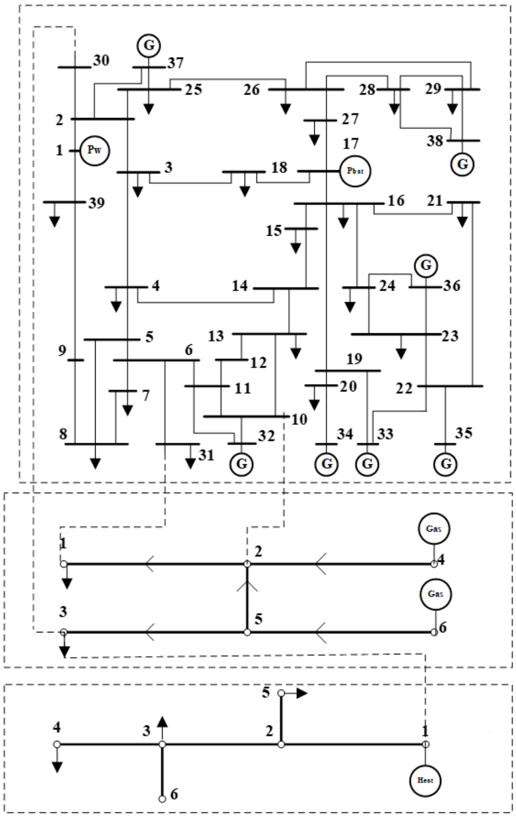

Figure 1: Topological diagram of Electric-Gas-Thermal interconnection integrated energy system

4.2 Analysis of simulation result

4.2.1 Normal scenario

In the normal scenario, the electric power system, gas system and thermal system are all in normal condition, and each load value is shown in Table. 1, with the unit being kW.

Table 1: Each load value in normal scenario

Pload1	Pload2	Pload3	Pload4	Pload5	Pload6
271.9114	393.2046	183.7857	379.4632	6.2573	215.8110
Pload7	Pload8	Pload9	Pload10	Pload11	Pload12
239.1199	128.0152	496.1179	185.0995	166.8385	224.3704
Pload13	Pload14	Pload15	Pload16	Pload17	Pload18
151.4061	93.7948	189.6647	149.7293	191.3248	6.2253
Pload19	Qload1	Qload2	Hload1	Hload2	Hload3
715.3201	176.2536	262.8035	26.4823	4.5061	18.0439

It can be seen from the table that the total electric load is 4387.4589kW, the total gas load is 439.0571kW, that is, 44.4222 m^3/h, and the total thermal load is 49.0323kW. The energy supply capacity of the Electric-Gas-Thermal interconnection integrated energy system under normal scenarios is 4875.5492kW.

4.2.2 Electric power system line N-1 fault scenario

Due to the complexity of the electric power system lines, this paper selects the first five cases with the maximum energy supply capacity for analysis, including: node 34, 20 line breaks, node 35, 22 line breaks, node 30, 2 line breaks, node 6, 31 line breaks, node 4, 14 line breaks.

Node 34, 20 line breaks, the output of generator 5 was interrupted, the output of wind turbine increased from 107.73kW to 150.87kW, the energy storage elements S_{ES} was reduced from 75kW to 60kW, the total electric load was reduced by 250.63kW, and the total gas load was reduced by 139.5714kW. The total thermal load increased by 10.1184kW, and the energy supply capacity was 4495.4653kW.

Node 35, 22 line breaks, the output of generator 7 was interrupted, the output of wind turbine increased from 107.73kW to 138.96kW, the energy storage elements S_{ES} was reduced from 75kW to 70kW, the total electric load was reduced by 250.63kW, and the total gas load was reduced by 89.9655kW. The total thermal load increased by 5.1071kW. The energy supply capacity is 4619.4207kW.

Node 30, 2 line breaks, and the CHP units could not provide electric energy to the electric power system. The total electric load decreased by 86.3756kW, the total gas load increased by 34.4672kW, the total thermal load decreased by 5.5979kW, and the energy supply capacity was 4818.0420kW.

Node 6, 31 line breaks, G2P device is interrupted, Pload18 is 0, the total electric load decreased by 53.8226kW, the total gas load increased by 27.8368kW, the total thermal load decreased by 1.2728kW, and the energy supply capacity is 4333.6363kW.

Node 4, 14 line breaks, the total electric load is reduced by 8.4477kW, the total gas load is reduced by 6.5445kW, the total thermal load is increased by 10.4691kW, and the energy supply capacity is 4379.0112kW.

4.2.3 Gas system line N-1 fault scenario

Gas system line N-1 fault scenario includes two scenarios: node 5, 6 line breaks, node 2, 5 line breaks.

Node 5, 6 breaks, gas source 2 is interrupted, and the total gas load is reduced by 198.7288kW, the total electric load is reduced by 220.5476kW, the total thermal load is reduced by 14.5522kW, and the energy supply capacity is 4441.7197kW.

Node 2, 5 breaks. At this time, the thermal system is disconnected, CHP units are interrupted, gas source 2 is interrupted, Hload1,2,3, Qload2 are all 0, the total electric load is reduced by 245.7684kW, the total gas load is reduced by 309.3817kW, the total thermal load is 0kW, and the energy supply capacity is 4271.3695kW.

4.2.4 Thermal system line N-1 fault scenario

Thermal system N-1 fault scenario includes two scenarios: node 2, 5 line breaks, node 2, 3 line breaks.

Node 2, 5 line breaks, Hload3 is 0, the total heat load is reduced by 15.5569kW, the total electric load is reduced by 33.6956kW, the total gas load is increased by 29.3172kW, and the energy supply capacity is 4855.6130kW.

Node 2, 3 line breaks, Hload1,2 is 0, the total heat load is reduced by 28.2492kW, the total electric load is reduced by 43.0752kW, the total gas load is increased by 49.9394kW, and the energy supply capacity is 4854.1385kW.

5. Conclusions

In this paper, the improved IEEE39-node power system, 6-node gas system and 6-node thermal system are used to verify the feasibility and effectiveness of the multi-scenario maximum energy supply capacity model of the Electric-Gas-Thermal interconnection integrated energy system with energy storage elements and wind turbines proposed in this paper. The experimental results show that the model can obtain the unique optimal solution, measure the maximum energy supply capacity, and provide decision support for the safe operation of the integrated energy system, more conducive to reasonable load distribution planning, and increase the reliability of the system operation. Subsequent modeling can add distributed power supplies such as photovoltaic and electric vehicles, and add more types of coupled devices, so that the modeling of the Electric-Gas-Thermal interconnection integrated energy system is more comprehensive and accurate. After perfecting the modeling, we can try to build the online maximum energy supply capability analysis software to improve the practicability and applicability.

ISSN 2522-3488 Vol. 8, Issue 4: 10-15, DOI: 10.25236/IJNDES.2024.080402

References

[1] Guo R, Wang F, Rhamdhani M, et al. Managing the surge: A comprehensive review of the entire disposal framework for retired lithium-ion batteries from electric vehicles[J]. Journal of Energy Chemistry, 2024, 92(05):648-680.
[2] Liu A, Zhang X, Liu Z , et al. The Roadmap of 2D Materials and Devices Toward Chips[J].Nano-Micro Letters, 2024, 16(06):349-444.
[3] Xin He. Research on Cooperative Optimal Scheduling and Benefit Balancing of Clean Energy Considering Multi-energy Complementation [D]. North China Electric Power University (Beijing), 2019.
[4] Dou Xun, Zhao Wenhao, Lang Yi Zihe, Li Yang, Gao Ciwei. A review of gas-power coupling system operation with power-to-gas technology [J]. Power System Technology, 2019, 43(01):165-173.
[5] Zheng Jieyun, Ni Shiyuan, Shi Pengjia, Wu Guilian, Wang Rian, Hu Zhijian. Calculation of Maximum Power Supply Capacity of Three-phase Unbalanced Distribution Network Based on Mixed Integer Second Order Cone [J]. Journal of Wuhan University (Engineering Science), 2020, 53(07):643-652.
[6] Jiu Cheng Z, Jie W, ShiZhong Z, et al. Application of ultrasonic fatigue technology in very-high-cycle fatigue testing of aviation gas turbine engine blade materials: A review [J]. Science China(Technological Sciences), 2024, 67(05):1317-1363.
[7] Gu Yuanyuan. Maximum Energy Supply Capability and Safety Grade Classification of Power - Gas Interconnection Energy System [D]. Yanshan University, 2019.
[8] DORCHEH F, M. GHASSEMI. The viscous strip approach to simplify the calculation of the surface acoustic wave generated streaming [J]. Applied Mathematics and Mechanics(English Edition), 2024, 45(04): 711-724.
[9] Wei Zhenbo, Ren Xiaolin, Huang Yuhan. Multi-objective optimization scheduling of regional integrated energy system considering comprehensive demand side response [J]. Electric Power Construction, 2020, 41(07):92-99.
[10] Ren J, Lou H, Xu N , et al. Methanation of CO/CO_2 for power to methane process: Fundamentals, status, and perspectives [J]. Journal of Energy Chemistry, 2023, 80(05):182-206.
[11] Tian Feng, Jia Yanbing, Ren Haiquan, et al. Integrated Energy system "source-load" low-carbon economic dispatch considering carbon capture System [J].Power Grid Technology, 2020, 44(09):3346-3355.DOI:10.13335/j.1000-3673.pst.2020.0728.
[12] LIU Ronhui, Li Yang, Yang Xiu, et al. Two-stage optimal scheduling of community integrated energy system considering demand response [J]. Acta Solar Energy Sinica, 2021, 42(09):46-54. (in Chinese) DOI:10.19912/ J.0254-0096.tynxb.2019-0974.